



NOVEL NANOSTRUCTURE ELECTROLYTIC MATERIALS

$Ba_{1-x}Sr_xCe_{0.4}Zr_{0.6}O_{3-\delta}$ FOR FUEL CELL APPLICATION.

M. M. Fukate¹, A. B. Bodade², G. N. Chaudhari³

Shri Shivaji science college , Nanotechnology Department Amravati.[M.S] India

Corresponding Author : manishfukate@gmail.com

ABSTRACT

In this paper the conductivity of nanostructured Sr doping effect of the novel $Ba_{1-x}Sr_xCe_{0.4}Zr_{0.6}O_{3-\delta}$ is investigated. The Sr doping affects in smaller grain size of nanocomposites and also restrain the making of secondary phase of $SrCeO_3$ in all various formulation of $Ba_{1-x}Sr_xCe_{0.4}Zr_{0.6}O_{3-\delta}$. The orthorhombic structure was detected with highest conductivity of 2.09×10^{-3} S/cm found at 600°C in $Ba_{0.95}Sr_{0.05}Ce_{0.4}Zr_{0.6}O_{3-\delta}$. The miniature lattice volume, better grain size, and lower activation energy that causes increase in conductivity in $Ba_{0.95}Sr_{0.05}Ce_{0.4}Zr_{0.6}O_{3-\delta}$ and $Ba_{0.75}Sr_{0.25}Ce_{0.4}Zr_{0.6}O_{3-\delta}$ shows lower conductivity with value of 4.70×10^{-4} S/cm in dry air at 600°C than Sr = X = 0.05 doped. The sol-gel synthesis method plays the important role in properties of electrolyte. Hence the formulation can be hopeful electrolyte if the sintering temperature, dopant concentration and time are controlled.

Keywords: SOFC, electrolyte, Pervoskite, Nanocomposite, Impedance

1.Introduction

For electrolyte application in fuel cell the barium cerate and strontium cerate are mainly used cerates they are the electro catalyst having large electro conductivity at elevated temperature [1-12]. The electrolyte material must have high protonic, mixed ionic, electronic conductivity, mechanical, chemical, and thermal stability, however protonic material yet not find out which is effective in all sense as described above.

So wide research is necessary in field of proton absorption and migration mechanism. Many researcher synthesized $BaCeO_3$ using various

methods such as solid state method, sol gel [13]. In contrast to $BaCeO_3$, $BaZrO_3$ chemical shows more stability in CO_2 atmosphere but have low proton conducting capacity [14,15]. But exhibit low proton conductivity. The solid state method have disadvantages as material prepared by this method needs calcinations temperature 1200°C followed by sintering at 1400°C , such prolonged calcinations and sintering result in crystal growth which obstacle the dense ceramic however they possess good electrical properties. The sol-gel method is used for preparation of sample. To have better homogeneity, greater reactivity. Most reliable method for making nanoparticle from the metal oxide is sol gel even at lower sintering temperature [16]. It is found that $SrCeO_3$ is more stable than $BaCeO_3$ [17] and up till now $BaSrCeZrO_3$ structure is not investigated by researcher as electrolyte material for fuel cell. The present work deals with the effect of strontium by partially proportionating with Ba in A site in Sr doped barium cerate Zirconates. The chemical stability and conductivity as electrolyte material for fuel cell which would be also used as base material for doping other dopant.

1.1 Characterization

The phase identification of the sintered oxides is analysed with a powder diffractometer (PANalytical X-pert Pro, Netherlands) with Ni filtered Cu-K α radiation and the diffraction angle from 10° to 90° with an interval of $0.010^\circ/\text{min}$. Morphologies of the sintered pellets are examined using scanning electron microscope (JEOL model JSM 6610 LV) in combination with an energy dispersion spectrometer (EDS) (INCA Energy 250, Oxford, UK) to estimate the percentage of elements present in the samples. By using an

HIOKI 3532-50 LCR HI-TESTER . Impedance range 50Hz-5MHz and at temperature range 37 measurement were carried out in the frequency to 600°C in air atmosphere.

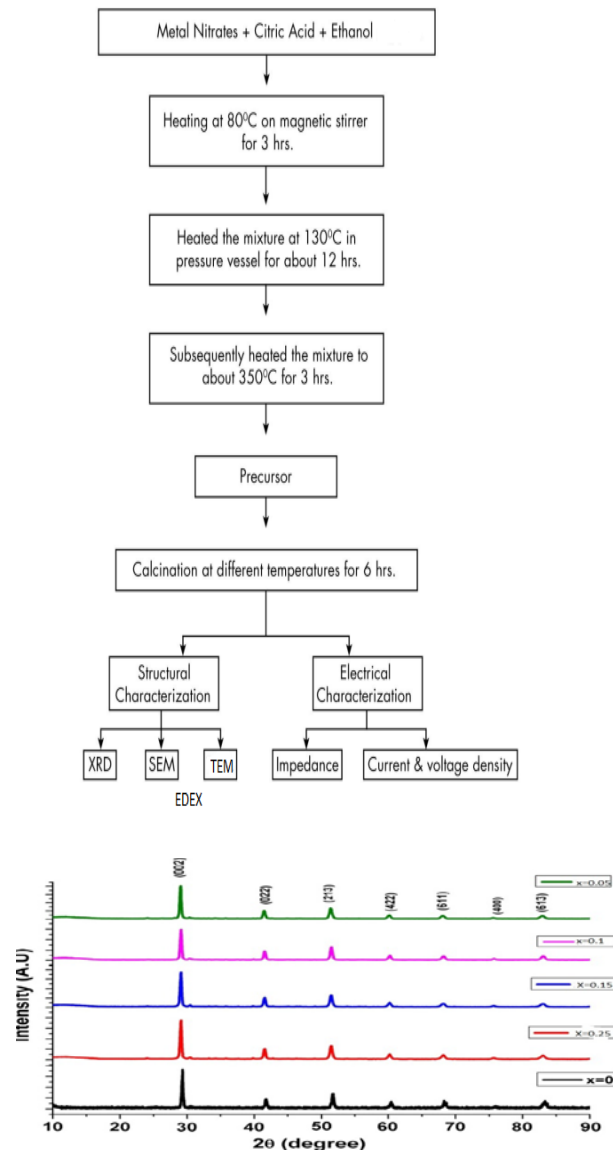


Fig : 1.1 XRD Pattern of sample $Ba_{1-x}Sr_xCe_{0.4}Zr_{0.6}O_{3-\delta}$ sintered at $800^\circ C$

1.2 Result and Discussion

1.2.1 XRD analysts:

Fig. 1.1 shows the XRD patterns of calcined at $350^\circ C$ for 5 hrs to remove the organic matter and then and sintered at $800^\circ C$ ceramic powders. The pattern reveals that it is single perovskite structure and having single phase with little impurities of $BaCeO_3$ and CeO_2 . The credit should be given to the sol-gel process where the pH is adjusted at 6 so more proton liberated from citric acid so as to increase the chelate formation process at comparatively less temperature, as a result phase formation is done.

The development of $BaCO_3$ contamination probably due to reaction between Ba^{2+} and Co^-

ions, formed due to reaction between citric acid and EDTA during heating on hot plate [23]. The small peaks seen are of $BaCO_3$, since those peaks are near by CeO_2 . As Sr doping is increased by 0.05 the CeO second phase is hindered. $Ba_{1-x}Sr_xCe_{0.4}Zr_{0.6}O_{3-\delta}$ oxides in all structures shows orthorhombic structure, with $pcmn$. The seven peaks are seen namely (0 0 2), (0 2 2), (2 1 3), (6 1 1), (4 2 2), (4 4 0), and (6 1 3) planes. The X-ray diffraction angles of $Ba_{1-x}Sr_xCe_{0.4}Zr_{0.6}O_{3-\delta}$ perovskite shifted to higher angles with increase in the Sr doping content and are the Sr doping content and are consistent with the investigations reported by Zeng. et al. [21,22]. Crystalline sizes of the powder were calculated using Scherrers formula

and a slight increase in the crystallite size was noticed from 29 nm ($Sr = 0.05$) to 31.3 nm ($Sr = 0.25$).

1.2.2 Scanning electron microscopy and EDAX analysis:

The SEM and TEM analysis (Fig 1.2) reveals that powder sintered at 800°C confirmed that the ceramic material is properly densified with very few pores which might be caused due to the vaporization of surface water and residual organics due to high sintering. From $x = 0.05$ to $x = 0.25$ the decrease in grain size is observed as Sr doping increased. To know the Sr doping result on structural stability, it is observed that very tiny size of barium atom is unable to stabilize the cubic perovskite structure

with given B site composition, The smaller Sr ion substituted in crystal lattice creates distortion and contribute to lowering of symmetry.

As a result the proton located near oxygen site is separated by high energy barrier. High temperature sintering may further enhance the density but BaO evaporation could be occurred. There may be chance of more BaO evaporation.

EDAX analysis Fig:1.3 is carried out to determine the elemental composition of powder. The confirmation is up to mark and analysis shows stoichiometric ratio without any detectable impurity confirmed that all elements are present in stoichiometric ratio.

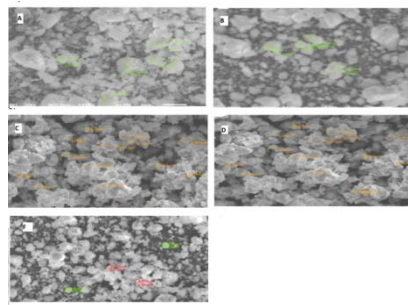


Fig 1.2 :SEM images of sintered samples of $\text{Ba}_{1-x}\text{Sr}_x\text{Ce}_{0.4}\text{Zr}_{0.6}\text{O}_{3-\delta}$ for a) $x=0.5$, b) $x=0.1$, c) $x=0.15$, d) $x=0.2$, e) $x=0.25$

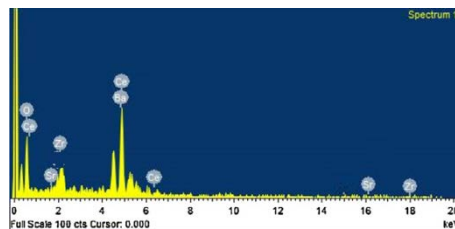


Fig 1.3 EDEX spectra of sintered samples of $\text{Ba}_{1-x}\text{Sr}_x\text{Ce}_{0.4}\text{Zr}_{0.6}\text{O}_{3-\delta}$ for a) $x=0.5$ sintered sample

1.3 Impedance measurements:

Electrolyte conduction greatly affects the overall energy performance of high-temperature solid oxide fuel cells. Here the ionic conductivity of $\text{Ba}_{1-x}\text{Sr}_x\text{Ce}_{0.4}\text{Zr}_{0.6}\text{O}_{3-\delta}$ is evaluated as a function of temperature in dry air atmosphere. The impedance spectra are measured from room temperature to 600°C . The temperature is confined to 600°C due to instrumental limitations and measurements at higher temperature are under process, which will be reported further. The spectra comprises of 3 arcs at high, medium and low frequencies corresponding to the interior of grain, grain boundary and the electrode, respectively [18,19]. In the Nyquist plots of the present work

as observed from Fig. 1.4, the high-frequency and low-frequency arcs are missing due to the instrumental limitations of temperature and frequency. Hence, the bulk response is assigned to the high-frequency intercept of the medium arc with the real axis, [20,21]. which depicted variations of about two to three orders of magnitude with rise in temperature from 30° to 600°C . The semi-circular pattern represents the electrical process taking place that can be expressed in an electrical circuit with a parallel combination of resistive and capacitive elements [24,25]

The frequency-dependent conductivity and dielectric permittivity studies yield important information on the ion transport and relaxation

studies of fast ionic conductors. EIS data can be represented in two basic formulas interrelated to each other, which are given below.

Complex impedance : $Z'' = Z' - jz''$

Complex permittivity : $\epsilon^* = \epsilon' - j\epsilon''$

$$\sigma_{ac} = \sigma_o \exp\left(\frac{-E_a}{K_b T}\right)$$

1.3.1 AC conductivity studies:

The electrical conductivity of synthesized compound is carried out over a frequency range of 50 Hz to 5 Mhz in temperature range of 50-600°C. The conductivity are found to be 10^{-4} s/cm at 600°C . Calculation of activation energy (Ea) The activation energy of all samples has been calculated at hydrogen atmosphere. Arrhenius curves have been plotted and shown in Fig. 1.5 and . These plots exhibit an increasing linear function of temperature, however, using the linear fit technique, the activation energies were calculated of all the materials by using formula given below

where Ea is activation energy sigma is the conductivity, T is temperature in kelvin, A is exponential factor, and K is Boltzmann's constant [26,27] The results of measurements of activation energy from AC conductivity at dry air .The activation energy of sample increased with Sr content which is determined from the graph. Sample with Sr content x=0.05 shows lowest barrier of activation energy and values confirmed that the sample is suitable to be used as electrolyte for fuel cell.

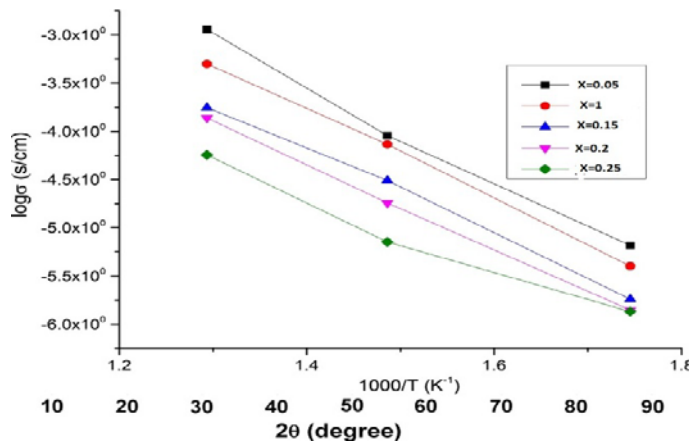


Fig 1.4 Nyquist plot sintered Ba_{0.95}Sr_{0.05}Ce_{0.4}Zr_{0.6}O_{3-δ} sample at 600°C

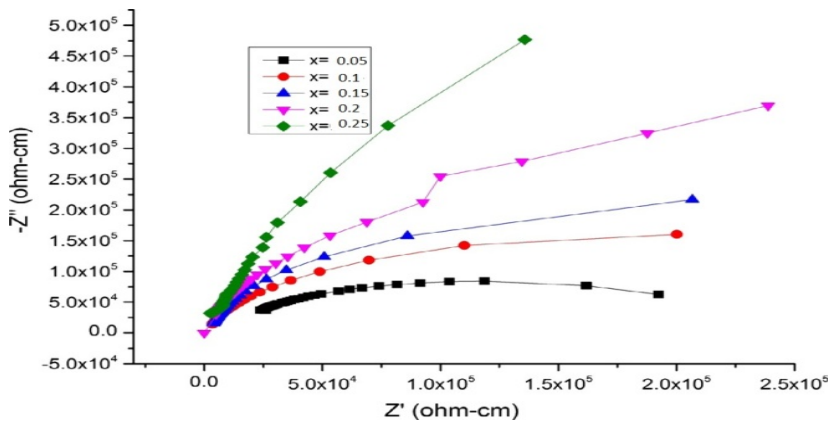


Fig 5.5 Arrhenius plot total conductivity of sample sintered Ba_{0.95}Sr_{0.05}Ce_{0.4}Zr_{0.6}O_{3-δ} in air atmosphere

1.3.2 Bode plots:

Nyquist plots are the first choice for EIS measurement but have drawback that they do not provide information regarding time or frequency. To avoid this problem, Bode plots can be analyzed. The variations of real (Z') and imaginary (Z'') parts of impedance with frequency measured at different temperatures are shown in Fig. 1.6. The Z' values decreased sharply with increase in frequency and display characteristic dispersion at low frequencies. The value of Z'' increased with a rise in frequency followed by a decrease and the peak positions shifted towards higher frequency side

along with peak broadening with rising temperatures as shown in Fig.1.7. The asymmetric broadening of peaks in Z'' vs. frequency entails that there is a spread of relaxation time, which indicates a temperature dependence electrical relaxation phenomenon in the material [26]. The peak in the lower frequency region may appear due to the electrode polarisation.

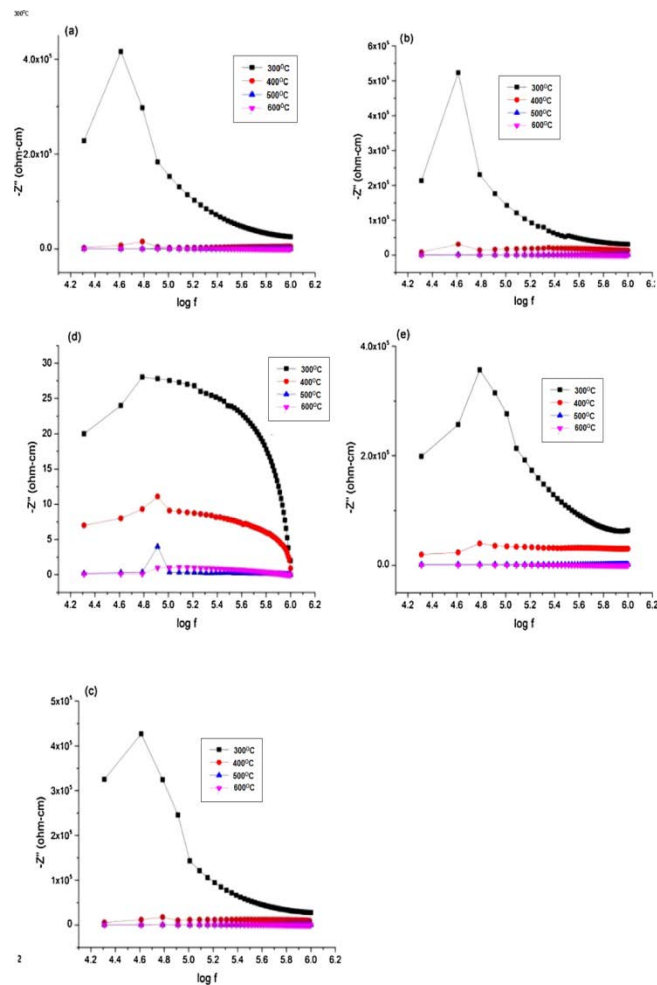


Fig.1.6 $Ba_{1-x}Sr_xCe_{0.4}Zr_{0.6}O_{3-\delta}$ ($x=0.05,0.1,0.15,0.2,0.25$) oxides sintered pellet at $800^\circ C/6$ h: (a) $x = 0.05$, (b) $x = 0.1$, (c) $x = 0.15$, (d) $x = 0.2$ and (e) $x = 0.25$.

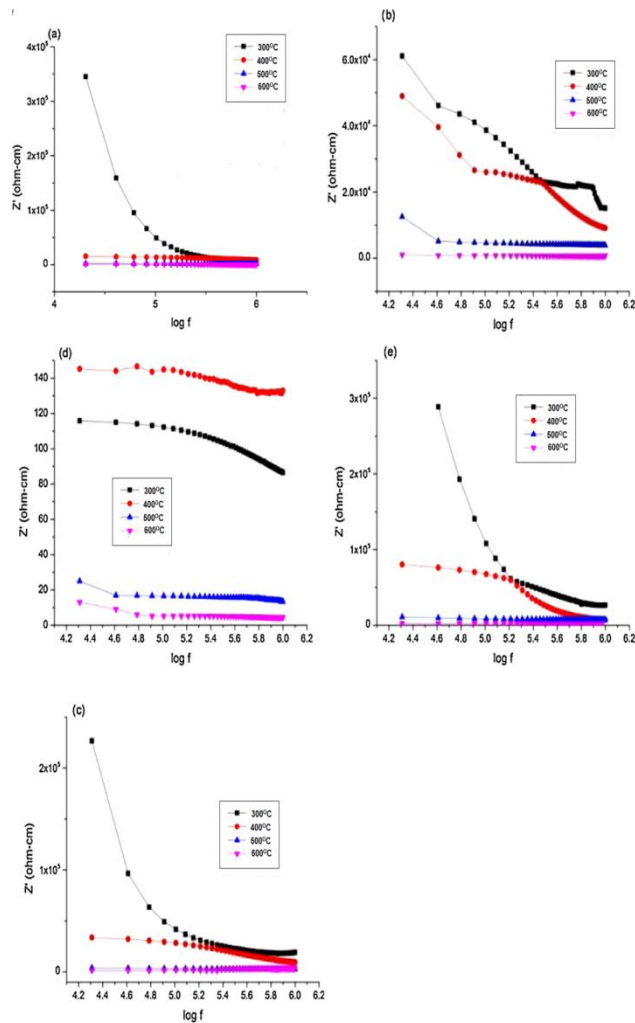


Fig. 1.7 Variation of Z'' with frequency of $\text{Ba}_{1-x}\text{Sr}_x\text{Ce}_{0.4}\text{Zr}_{0.6}\text{O}_{3-\delta}$ ($x=0.05,0.1,0.15,0.2,0.25$) oxides sintered pellet at $800^\circ\text{C}/6\text{ h}$: (a) $x = 0.05$, (b) $x = 0.1$, (c) $x = 0.15$, (d) $x = 0.2$ and (e) $x = 0.25$.

1.4 Conclusion

The study logically present the relationship between Sr doping content and nanostructure chemical stability and structural analysis of $\text{Ba}_{1-x}\text{Sr}_x\text{Ce}_{0.4}\text{Zr}_{0.6}\text{O}_{3-\delta}$. The electrolyte prepared by sol gel method. Single phase perovskite nanostructure $\text{Ba}_{1-x}\text{Sr}_x\text{Ce}_{0.4}\text{Zr}_{0.6}\text{O}_{3-\delta}$. It is observed that Doping of Sr into the composite resulted in smaller grain size and also suppresses the formation of SrCeO_3 same as second phase. The $\text{Ba}_{0.95}\text{Sr}_{0.05}\text{Ce}_{0.4}\text{Zr}_{0.6}\text{O}_{3-\delta}$ Nanocomposite shows orthorhombic structure highest conductivity with value of $2.10 \times 10^{-3} \text{ s/cm}$ at 600°C due to its smaller activation energy. $\text{Ba}_{0.75}\text{Sr}_{0.25}\text{Ce}_{0.4}\text{Zr}_{0.6}\text{O}_{3-\delta}$ recorded lower conductivity with value of $4.72 \times 10^{-4} \text{ s/cm}$ at 600°C . All Nanocomposite gives good chemical stability at every temperature. The Bode plot shows the temperature dependence

electrical relaxation phenomenon in material. Comparison in literature showed the importance of the synthesis methods on the properties of nanocomposite. The study elucidates that $\text{Ba}_{1-x}\text{Sr}_x\text{Ce}_{0.4}\text{Zr}_{0.6}\text{O}_{3-\delta}$ is promising electrolyte and for the use as SOFC if the Sr doping is limited to small amount

1.5 References:

1. Haile S M, Staneff G, Ryu KH. Non-stoichiometry,. J Mater Sci 36 (2001) 1149-1160.
2. Hermet J, Bottin F, Dezanneau G, Geneste G.. Phys Rev 87 (2012) 104-115.
3. Tania P, Kanwar Gulsher Singh P, Thangadurai V.. Inorg Chem, 47 (2008) 8972-84.
4. Zhao F, Chen F Int JHydrogen Energy;35(2010) 11194–11199

- Ivanov MG, Shmakov AN, Drebushchak VA, Podyacheva Oyu. 100 (2010) 79-82.
5. Tong J, Clark D, Bernau L, Subramaniyan A, Hayre. Solid state Ion 181 (2010) 1468 -1498.
 6. Bi L, Tao Z, Liu C, Sun W, Wang H, Liu W.J Memb Sci 336 (2009) 1-6.
 7. Zhahriev A, Kaloyanov N, Girginov C, Paranova V. Acta Chemica 528 (2012) 85-99.
 8. Iwahara H, Uchida H, Morimoto K.. J Electrochem Soc; 137 (1990) 462-472.
 9. Kwang HR, Haile SM. Solid State Ion,125 (1999) 355–367.
 10. Fanglin C, Ping W, Sorensen OT, Meng G, Peng D.. J Mater Chem 7 (1997) 1533–1539.